#566: Exploiting environmental energy and waste heat with joint circulation systems

Mathias FRAAB[1]

[1] Berliner Hochschule für Technik

Abstract: Joint Circulation systems (JCS) are used for heat recovery in air conditioning systems. Additional water/water heat exchangers inside the circulation can substitute air heaters and air chillers. Due to their significantly lower temperature differences aggregates like heat pumps can be operated at good performance coefficients, similiarly as with thermoactive slabs. These JCS also provide the opportunity to extract waste heat from the return air which would otherwise escape with the exhaust air. This paper introduces design rules for these JCS under different operating modes.

Keywords: Joint Circulation Systems, Balanced Building Climatization Technology, Feeding in Heating and Cooling EnergyInside the Circulation, Capillary Tube Technology, Laminar Flow Through a Parallel Gap

1. INTRODUCTION

JCS were widely introduced to the market in the 1970s. They are for choice when supply and return air should be separated to the highest extent possible. The first guideline to include them was VDI 2071 [1] which meanwhile has beenremoved. The integration of their control into the control of air handling units was introduced in VDI 3525 [2]. Beginning with VDI 3803 (5) [3] JCS with water/water heat exchangers inside the circulation were dealt with in German guidelines. With DIN EN 13053 JCS found their way into European standardization.

Jüttemann [5] showed how to calculate the heat recovery coefficient of the JCS from the heat recovery coefficients of the single air/water heat exchangers. Due to the reduction of heat recovery coefficient of the JCS compared with the heat recovery coefficients of the air/water heat exchangers, a demand for high efficiency heat exchangers has arisen. At first, it was met by heat exchangers made from copper with baffles between the pipes and small gaps between the baffles leading to laminar heat flow. It was only based on this performance that multifunctional JCS became an option as described by Kaup [5].

Another way to construct high efficiency heat exchangers is by use of polypropylene. D. Herbst, the inventor of capillary tube mats, developed new flat mats with cross-linked pipes for this purpose [7]. JCS with these heat exchangers were subject of the research project katube.X-changer [8]. The mutual results of this project were reported by Kretschmer [9], [10] and Fraaß [11], in the latter case with respect to some similarities between multifunctional JCS and thermoactive slabs based on the understanding of thermal activation as a field of temperature differences as described in [12].

This paper aims at closing the gap between basics and applications by extending this comparison to application fields in a technical surrounding shaped by environmental temperature potentials and the need to deploy aggregates like heat pumps with high efficiency. In this context some operation modes will be discussed. After clarifying the basics, a set of formulas will be set up, calculations will be carried out and the results will be discussed.

2. JCS WITH EXTENDED FUNCTIONS

Figure 1 shows on the left a conventional JCS which serves only for heat recovery and on the right a system with extended functions provided by two water/water heat exchangers referred to as inner link and outer link.

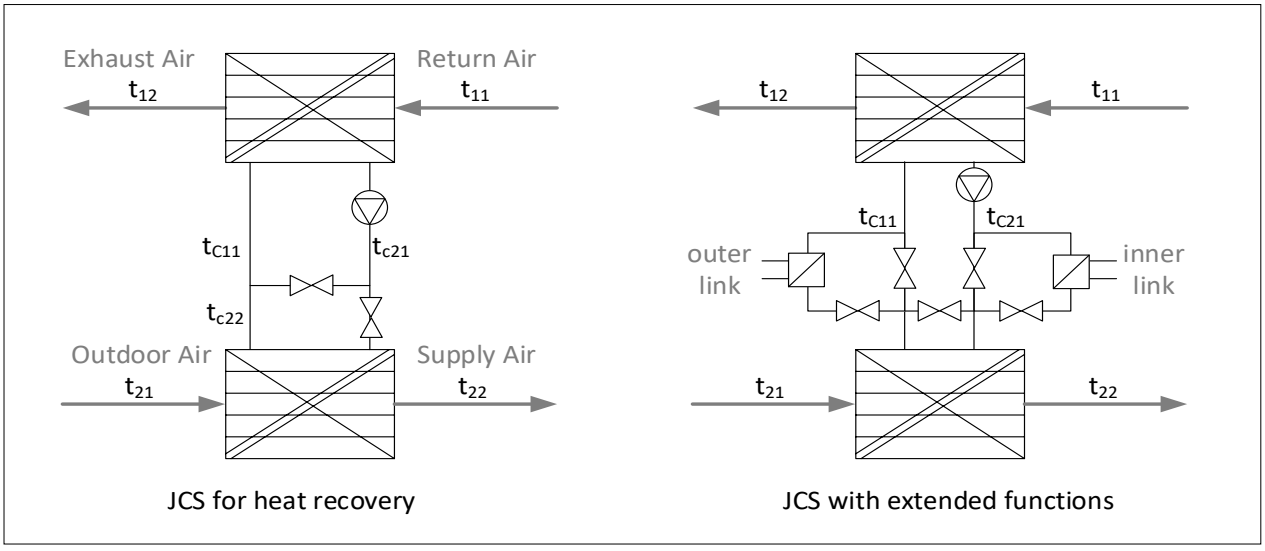

Figure 1: Circular interconnected system

By means of the circulation system the return air heats the outdoor air when lower than the return air. Otherwise, the outdoor air is cooled. In order to prevent damages of the exhaust air heat exchanger from water temperatures t_{C11} below the freezing point water from the outdoor heat exchanger with the temperaturet_{C22} is mixed with water from the inner side of the circulation with the temperature t_{C21}. During these periods the efficiency of the heat recovery is restricted.

In the extended system the outer link is used to feed in heat at temperatures which are low but higher than the freezing point. Here, the bypass is used only in emergency cases. Apart from that the heat recovery remains unrestricted. The inner link is used for feeding in heat and extracting heat as well. The operation mode changes by the positions of additional valves not shown in the figure.

Figure 2 shows some operation modes in technical surrounding with solar collectors on the roofs, long-term storages inthe cellar or in the soil beneath the buildings and a common anergy grid for a district which as well may contain deep boreholes more than 100 m deep for extended geothermal exploitation. The buildings are linked to the anergy net both byheat exchangers and heat pumps which can also operate in cooling mode.

Partial figure 1 shows the aforementioned operation mode with natural frost protection during periods with outdoor temperatures below the freezing point. In order to avoid damage of the exhaust air heat exchanger the anergy grid is unloaded. Thus, the JVS can run with maximum efficiency even during frost periods.
In Partial figure 2 the heat pump is deployed for heating via the inner link. Typical temperature pairs at air heaters are 60/40 or even 80/60. At these temperatures heat pumps would run with low efficiency. Due to the much lower mean temperature differences in the inner links efficiency is significantly increased. This is similar to deploying thermoactiveslabs instead of radiators.

Partial figure 3 shows the loading of a long-term storage with solar thermal heat while partial figure 4 shows its unloading. At the same time the heat from the solar collector is fed into the anergy grid. The long-time storage is designated for higher temperatures than the anergy grid so that it can heat via the JCS and/or thermaoactive slabs directly instead deploying the heat pump.

Partial figure 5 shows cooling via the inner link with the heat pump running in cooling mode, thus transferring heat into the anergy grid. While 6/12 is a typical temperature pair at air chillers the inner link is also deployed with much lower temperature differences between the media when cooling, this enhancing the efficiency of the heat pump in cooling mode.

These low temperature differences also make it possible to use the anergy grid for cooling during at high outdoor temperatures, as partial figure 6 shows. This is possible over much longer periods than free heating would be possible.It is the same operation mode when waste heat from the return air is extracted via the inner link and fed into the anergy grid during any period of the year.

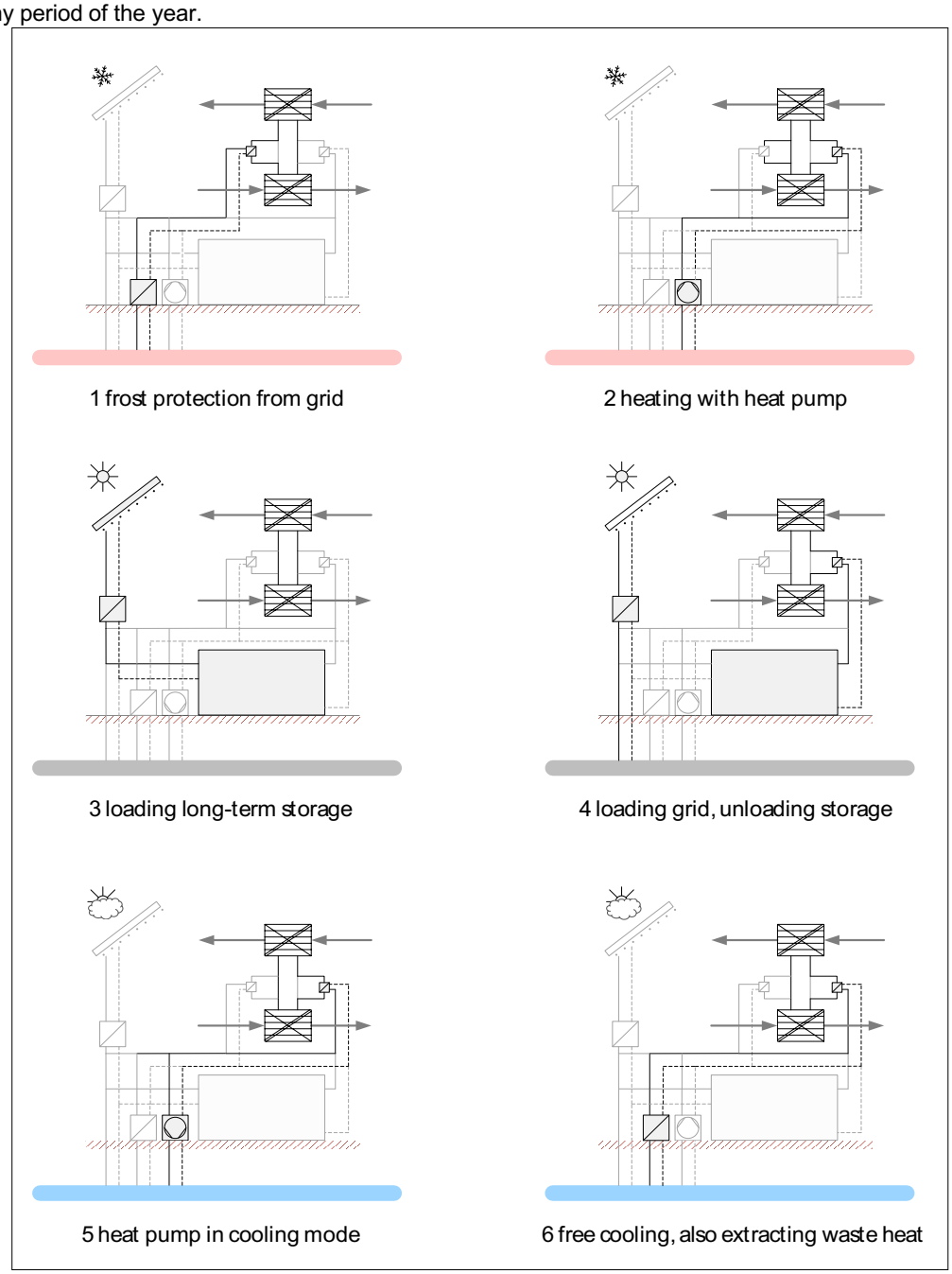

Figure 2: Operation modes

3. COUNTER FLOW HEAT EXCHANGE

All heat exchangers in the JCS are counterflow heat exchangers. **Figure 3** shows on the left the counterflow principle with two capacity flows C_1 and C_2 heading in opposite directions on both sides of the separating face of the heat exchanger. The first index of the temperatures denotes primary side (1) or secondary side (2). The second index denotes inlet (1) or outlet (2). On the right temperature courses of the two media are shown when C_2 equals C_1 case.

With the ratio between the capacity flows

(1) $\mu = \frac{\dot{C}_2}{\dot{C}_1}$

the reference case is μ = 100%. In this case the mean temperature difference Δt between the media equals a minimum value

(2) $\Delta t_{min} = t_{12} - t_{21} = t_{11} - t_{22}$

of the temperatures involved, whereas

(3) $\Delta t_{max} = t_{11} - t_{21}$

serves as a maximum value to be related to. With these temperature differences the nominal value Φ_{100} of the heat recovery coefficient at μ = 100% is

(4) $\Phi_{100} = 1 - \frac{\Delta t_{min}}{\Delta t_{max}}$.

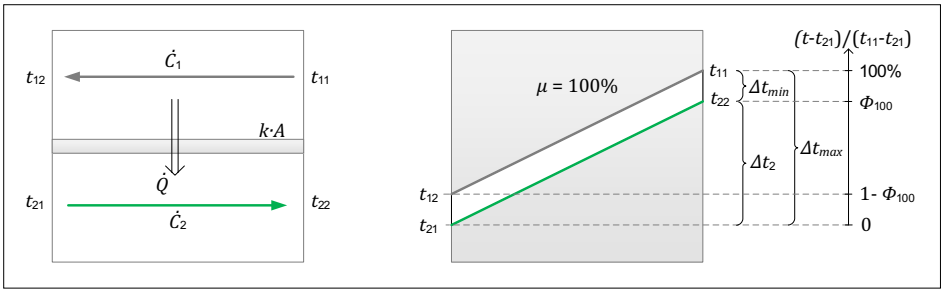

Figure 3: Heat transfer in counter flow heat exchangers at equal capacity flows

With given media it mainly depends on the area A of the separating face. Along with the heat transfer coefficient k between the media the transferred heat $\dot{Q}$100 at μ = 100% is

(5) $\dot{Q}_{100} = k\ A\ \Delta t_{min}$.

On the secondary side it can also be calculated as

(6) $\dot{Q}_{100} = \dot{C}_2\ \Delta t_2$

With

(7) $\Delta t_2 = t_{22} - t_{21} = \Delta t_{max} - \Delta t_{min}$.

With these correlations the number of transfer units is

(8) $\mathrm{NTU} = \frac{k\ A}{\dot{C}_2} = \frac{\dot{Q}_{100}/\Delta t_{min}}{\dot{Q}_{100}/(\Delta t_{max} - \Delta t_{min})} = \frac{1-\frac{\Delta t_{min}}{\Delta t_{max}}}{\frac{\Delta t_{min}}{\Delta t_{max}}} = \frac{\Phi_{100}}{1-\Phi_{100}}$.

Therefore Φ_{100} can also be written as

(9) $\Phi_{100} = 1 - \frac{1}{1+\mathrm{NTU}}$.

This equation makes clear how Φ_{100} depends on the size of the heat exchanger contained in the NTU. Table 1 shows pairs of NTU and efficiency that arise when the degree is continuously halved

Table 24: Dependency of Φ_100 on the NTU

NTU	Φ_{100}
1.5	60%
4	80%
9	90%
19	95%

The associated values of $\Delta t_{min}/\Delta t_{max}$ are 40%, 20%, 10% and 5%. One might expect that the NTU and with it the area A must be doubled in order to halve $\Delta t_{min}/\Delta t_{max}$. Figure 4 shows why the area has to be more than doubled in order to halve $\Delta t_{min}/\Delta t_{max}$ from 20% to 10%.

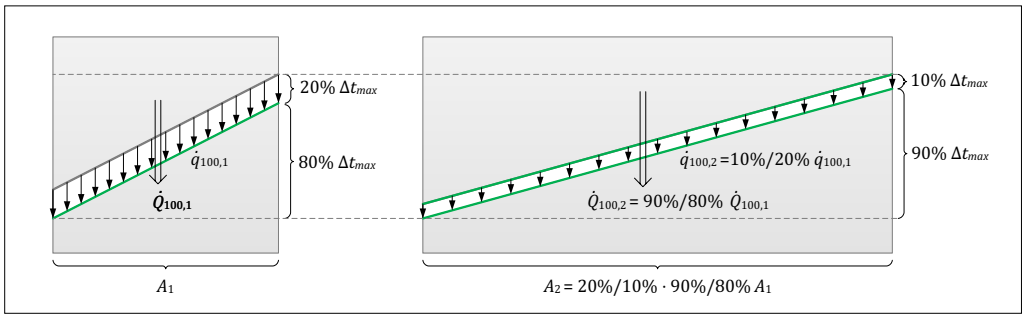

Figure 4 *Dependency of Φ_{100} on the area A of the separating face*

Due to the halved temperature difference Δt_{min} the density of the heat flow $\dot{q}_{100} = k\,\Delta t_{min}$ has been halved, too. Only if $Q_{100} = A\ \dot{q}_{100}$ was constant, A would have in fact to be doubled. However, due to the higher coefficient of performance Q_{100} increases by a factor 90%/80% = 1.125. Therefore, the size of the heat exchanger increases by 2.25 to become Φ_{100} = 90%.

To get an idea of the size of the separating face here is an example for an air flow of 9,000 m³/h related with a capacity flow $C_{\dot{2}}$ = 0.34 · 9,000 W/K ≈ 3,000 W/K If the heat transfer coefficient k can reach 40 W/(m² K) the size for Φ_{100} = 80% which means NTU = 4 will be A = 4 · 3,000 W/K / 40 W/(m² K) = 300 m². In order to achieve Φ_{100} = 90% which is NTU = 9 the size of the separating face must reach an amount of 675 m². This raises the question of what dimensions are involved.

4. HIGH EFFICIENCY HEAT EXCHANGER

Figure 5 shows on the left a commercially available heat exchanger made from copper as dealt with by Kaup [6] and on the right heat exchanger with capillary tube mats developed in the research project katube.X-changer [8]. The 1 EUR coin shows the fine structure of these mats.

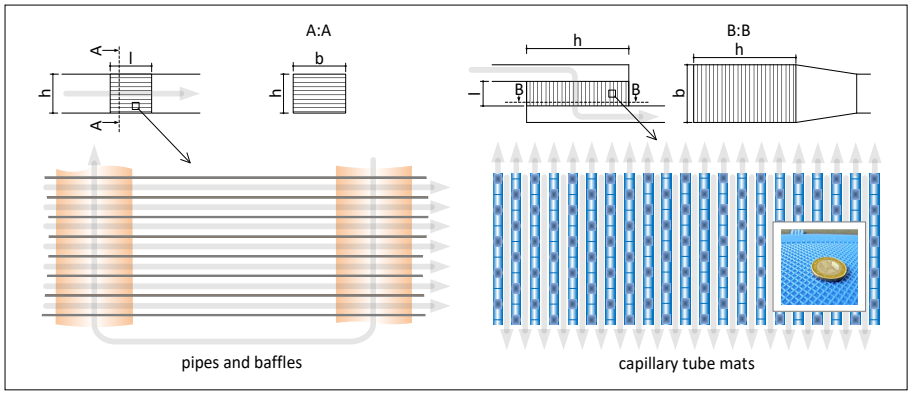

Figure 5: Layered laminary counterflow heat exchangers

The copper pipes are arranged at right angles to the air flow. The water flow is at the air outlet and the return flow is at the air inlet. The counterflow principle is realized here in a limited way by the temperature curves in the baffles as shown in the longitudinal section above along the length l of the heat exchanger. The cross section has width b and height h. In order to increase the size of the heat exchanger additional packs of length l must be installed, thus increasing the pressure drop.

The capillary tube mats are arranged vertically with air ducts above and beneath the heat exchanger. The length l in the flow path is limited to a value at which the pressure drop does not exceed a value of 50 Pa. This is to prevent good thermal

performance being achieved at the expense of high energy consumption for the fans. While the width of the mats l corresponds to the width oft he ducts the size oft he separating face is changed with the height h of the stack of mats and therefore with the number of mats giving air handling units a radically different appearance with the high efficiency heat exchangers as their main part.

As seen before, the size of the separating face A corresponds with the heat transfer coefficient k in the product $k\,A$. This raises the question of which values of k are possible. For an air/water heat exchanger, a useful representation of the heat transfer coefficient is

(10) $k = \frac{1}{r_f + r_p + \frac{1}{\alpha}} = a_2\,\alpha.$

r_p and r_f are the thermal resistances of the heat transfer in the mat and the heat transfer in the circulation medium. They also include the geometry of the mats. Typical values of the sum of r_p and r_f are between 3 10^{-3} and 5 10^{-3} m² K/W.

α can be calculated as

(11) $\alpha = a_1\,Nu\,\frac{\lambda}{d}$

with a_1 as a shape factor taking account of deviations from the shape of a parallel gap that can be determined by measurements. Values for Nußelt`s number for the parallel gap were given from 3.77 [13] up to 4.12 which was determined in own calculations. For instance, if $a_1\,\mathrm{Nu}$ = 4 and d = 2 mm at λ = 0,025 W/(m K), α will be 50 W/(m² K) as assumed before.

If the width of the mats is b = 1000 mm and the mean velocity of the air is w = 2.5 m/s, the flow through each gap between two mats will be 18 m³/h at d = 2 mm. For an airflow of 9,000 m³/h as assumed above 500 gaps are needed. If each mat has a thickness of 3.4 mm the height of the stack of the mats will be h = 500 (2 + 3.4) mm = 2700 mm.

The length of the mats corresponds with the pressure drop in the parallel gap by

(12) $\Delta p = a_3\,12\,\frac{\eta\,l\,w}{d^2}.$

a_3 is another shape factor for the deviation from the parallel gap, η is the viscosity of air. With a_3 = 1.1, η = 18 10^{-6} kg/(m s) at 20 °C, l = 675 mm and w = 2.5 m/s and d = 2 mm as assumed before, Δp will have a value of 100 Pa.

Thus, the resulting heat exchanger with Φ_{100} = 90% and Δp = 100 Pa for an air flow of 9,000 m³/h has a length of 2.7 m at a width of 1 m and a height of 0.675 m with the air ducts and also the water distributors and collectors above and beneath it.

If the length was doubled to 5.4 m, the heat recovery coefficient would be Φ_{100} = 95% and the pressure drop would be 50 Pa. These are new dimensions both in performance and appearance. This is why heat exchangers of these dimensions would significantly change the look of an air handling unit.

So far only the reference case μ = 100% was considered. Figure 6 shows on the left the dependency of the heat recovery coefficient Φ on the ratio μ of capacity flows. Φ_{100} = 90% is reached at μ = 100%. Higher values of μ increase Φ up to 100%. In the middle and on the right temperature courses inside the heat exchanger are shown at μ = 88% and μ = 133%.

The values of the courses are related temperatures of the form $(t - t_{21})/(t_{11} - t_{21})$ as already used in figure 3 on the very right. The reference case μ = 100% is highlighted in gray. The ends of the blue courses mark $(t_{22} - t_{21})/(t_{11} - t_{21})$ and therefore the achieved values of Φ as shown in the course of Φ on the left of figure 6 for μ = 88% and μ = 133%.

When μ is lower than 100% the primary medium 1 cools down stronger on its way to the outlet. So, both courses are bent downwards to the right. When μ is higher than 100% the primary medium cools down weaker on its way to the outlet. Thus, both courses are bent upwards to the left.

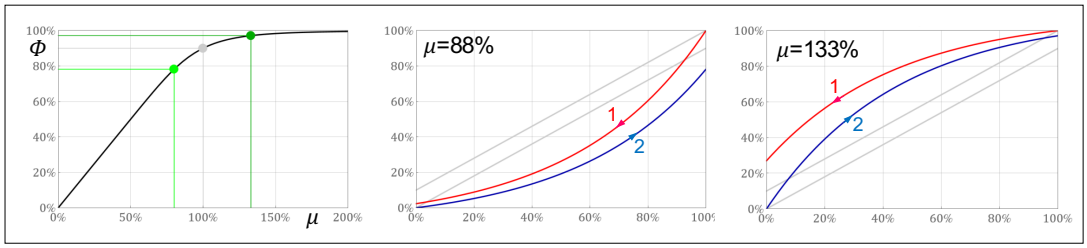

Figure 6: Dependency of Φ on the ratio μ of capacity flows

The values of the courses are related temperatures of the form $(t - t_{21})/(t_{11} - t_{21})$ as already used in figure 3 on the very right. The reference case μ = 100% is highlighted in gray. The ends of the blue courses mark $(t_{22} - t_{21})/(t_{11} - t_{21})$ and therefore the achieved values of Φ as shown in the course of Φ on the left of figure 6 for μ = 88% and μ = 133%.

When μ is lower than 100% the primary medium 1 cools down stronger on its way to the outlet. Thus, both courses are bent downwards to the right. When μ is higher than 100% the primary medium cools down weaker on its way to the outlet. So, both courses are bent upwards to the left.

5. HEAT RECOVERY IN THE JCS

Figure 7 shows the entire JCS with its two heat exchangers and the circulation (index C) between them. The heat exchangers are assumed to have the same size. Now, their heat recovery coefficient Φ_{100} has to be distinguished from the heat recovery coefficient $\Phi_{JCS,100}$ of the entire JCS. In the same way the maximum and minimum temperature differences have to be distinguished.

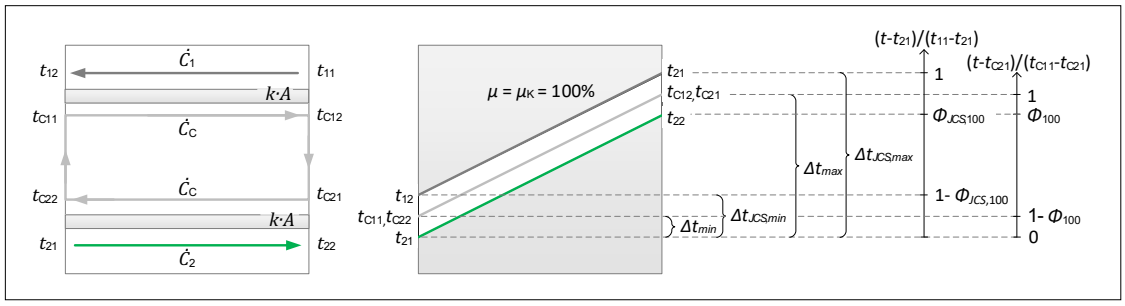

Figure 7: Heat transfer in the JCS at equal capacity flows

It can be seen from the figure that the maximum temperature difference $\Delta t_{JCS,x}$ of the JCS is $\Delta t_{max} + \Delta t_{min}$ whereas the minimum temperature difference $\Delta t_{JCS,min}$ of the JCS is $2 \cdot \Delta t_{min}$. Analog to equation (4) the heat recovery coefficient $\Phi_{JCS,100}$ of the JCS is $1 - \Delta t_{JCS,min}/\Delta t_{JCS,max}$. Expressed with the temperature differences of the heat exchangers this gives

$$(13)\ \Phi_{JCS,100} = 1 - \frac{2\,\Delta t_{min}}{\Delta t_{max}+\Delta t_{min}} = \frac{\Delta t_{max}-\Delta t_{min}}{\Delta t_{max}+\Delta t_{min}} = \frac{1-\frac{\Delta t_{min}}{\Delta t_{max}}}{1+\frac{\Delta t_{min}}{\Delta t_{max}}} = \frac{\Phi_{100}}{2-\Phi_{100}}.$$

Table 2 shows pairs of NTU and efficiency that arise when the degree is continuously halved

Table 2: Heat transfer coefficient of the entire JCS

NTU	Φ_{100}	$\Phi_{JCS,100}$
1.5	60%	43%
4	80%	67%
9	90%	82%
19	95%	90%

With the heat recovery coefficient Φ_{100} = 90% as in the above examples the heat recovery coefficient $\Phi_{JCS,100}$ of the entire JCS is only 82%. This is the reason why heat exchangers for JCS demand large separating faces and therefore also large dimensions.

The capacity flow to be changed in order to change the heat recovery coefficient of the JCS is the capacity flow of the circulation $\dot{C}_C$. Related to the capacity flow of the outdoor air this gives a ratio.

$$(14)\qquad \mu_C = \frac{\dot{C}_C}{\dot{C}_2}.$$

Another ration would be the ratio of the air flows

(15) $\mu_1 = \frac{\dot{C}_1}{\dot{C}_2}.$

To keep things simple, it is assumed to be μ_1 = 1 in the following unless otherwise stated.

Figure 8 shows on the left the dependency of the heat recovery coefficient Φ_{JCS} on the ratio . The heat recovery coefficients of the air water heat exchangers are supposed to be Φ_{100} = 95%, so Φ_{JCS} is 90%. This value is reached at μ_C = 100%. In the JCS both lower and higher values of μ_C decrease Φ_{JCS} as shown for μ_C = 88% in the middle and μ_C = 133% on the right. The reference case μ_C = 100% is again highlighted in grey.

At μ_C = 133% there is a part of the separation surface over which the water temperature in the outdoor heat exchanger is higher than the water temperature in the exhaust air heat exchanger. This does not mean that the heat transfer is reversed. In the outdoor heat exchanger the water temperature is still higher than in the air. And in the exhaust air heat exchanger the air temperature is still higher than the water temperature. Furthermore, the water outlet temperature t_{C12} of the exhaust air heat exchanger would match the water inlet temperature t_{C21} of the outdoor air heat exchanger and so would do t_{C22} with t_{C11}, if the circulation was perfectly insulated. But between these inlets and outlets it is perfectly possible that the water temperature in the outdoor heat exchanger can exceed the water temperature in the exhaust air heat exchanger. This is the reason why Φ_{JCS} decreases at higher ratios of the circulation flow than μ_C = 100%.

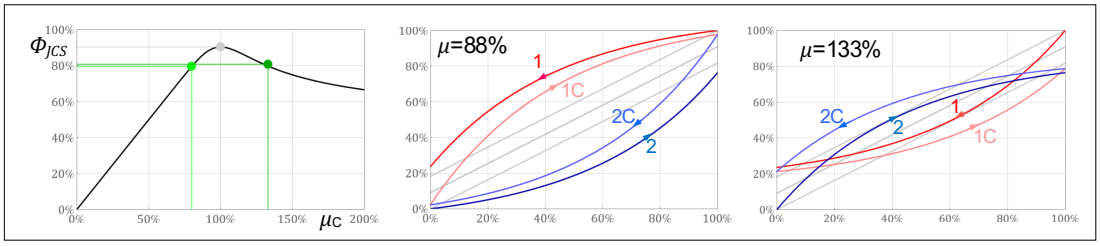

Figure 8: Dependency of Φ_{JCS} on the ratio μ_C of capacity flows

This raises the requirements for the control of the JCS. At first it is advisable to install temperature sensors at inlet or outlet, be it water or air. The optimum value μ_C = 100% ist reached when $t_{C21} - t_{C22} = t_{22} - t_{21}$ at μ_1 = 1. Otherwise $t_{C21} - t_{C22}$ must match the arithmetic mean of $t_{22} - t_{21}$ and $t_{11} - t_{12}$. The ratio of the flows is indirect proportional to the ratio of the temperature differences. Thus, a flow meter inside the circulation is enough to determine also the air flows which would pose serious measuring problems otherwise.

6. HEATING AND COOLING VIA THE INNER LINK

So far pure heat recovery has been regarded. Now it is accompanied by feeding in heating or cooling performance. This requires new calculation rules. Calculations become easier when heat recovery and feed-in are regarded separately. This is similar to the calculation of thermoactive slabs. Figure 9 shows the similarities in calculating both of them. In the thermoactive slab the source system consists of pipes that could also be capillary tube mats, for example.

Without the source system the termoactive slab is in a passive state and there ist only a heat transfer from inside to outside with a temperature profile between the temperature $t_{si,0}$ at the interiorr surface and the temperature $t_{se,0}$ at the exterior surface. The heat flows are related to the interior surface area A_s of the thermoactive slab as $\dot{q}_x = \dot{Q_x} / A_s$ with Q_x as the absolute heat flow.

With the source system in operation the thermoactive slabs change to an activated state. All temperatures t_x of the activated state can be written as

(16) $t_x = t_{x,0} + \Delta t_x.$

All heat flows of the activated state can be written as

(17) $\dot{q}_x = \dot{q}_{x,0} + \Delta\dot{q}_x$ rsp. $\dot{Q}_x = \dot{Q}_{x,0} + \Delta\dot{Q}_x.$

Because the passive state can easily be calculated, it is convenient not to calculate temperatures t_x and heat flows $\dot{q}_x$ of the activated state, but to calculate the difference variables Δt_x and $\Delta\dot{q}_x$. By use of the superposition principle the variables of the passive state can be added in order to get the variables of the activated state. In [12] the field of $\Delta t_x$is referred to as the activation, $\Delta\dot{q}_x$ are referred to as activation performances. The activation holds its positive sign also in cooling. In this case the variables of the activation must be subtracted from the variables of the activated state.

On the bottom of figure 9 the activation is shown for itself. It has homogeneous boundary conditions. This facilitates the

calculation of the two-dimensional field which is posed by the source system by making it unnecessary to calculate fields under equal and unequal temperatures on both sides of the thermoactive slab as in the activated state.

The only variable which remains the same in the activated mode and in the activation ist the source heat flow $\dot{q}$. The equivalent heat flows in the JCS are the heat flow Q_i via the inner link and $Q_e^{\cdot}$ via the outer link. It remains the same whether the pure feed-in is considered or the superposition heat recovery+feed-in with the pure heat recovery. Homogeneous boundary conditions exist here only at the inlets.

While it is more convenient with a thermoactive slab to first calculate the activation in order to determine the activated state from it, the reverse procedure is advisable with the JCS, i.e. to first calculate recovery + feed-in in order to obtain the feed-in by subtracting the recovery.

In figure 9 the following relations can be seen for recovery+feed-in:

(18) $\dot{Q}_i = \dot{C}_2\,(t_{C21} - t_{C12})$
$\dot{Q}_e = \dot{C}_2\,(t_{C11} - t_{C22})$
$\dot{Q}_1 = \dot{C}_2\,(t_{C11} - t_{C12})$
$\dot{Q}_2 = \dot{C}_2\,(t_{C21} - t_{C22})$
$t_{C22} = t_{C21} - \Phi_{100}(t_{C21} - t_{21})$
$t_{C12} = t_{C11} + \Phi_{100}(t_{11} - t_{C11})$

Together with equation (12) this yields at first with Q_e = 0:

(19) $\dot{Q}_2 = \frac{1+\Phi_{JCS,100}}{2}\,\dot{Q}_i + \Phi_{JCS,100}\,\dot{C}_2\,(t_{11} - t_{21}),\quad \dot{Q}_1 = \frac{1-\Phi_{JCS,100}}{2}\,\dot{Q}_i + \Phi_{JCS,100}\,\dot{C}_2\,(t_{21} - t_{22}).$

The second terms on the side are $\dot{Q}_{2,0}$ and $\dot{Q}_{1,0}$. So the heat flow $\dot{Q}$ is divided according to

(20) $\frac{\Delta\dot{Q}_2}{\dot{Q}_i} = \frac{1+\Phi_{JCS,100}}{2}$, $\qquad \frac{\Delta\dot{Q}_1}{\dot{Q}_i} = \frac{1-\Phi_{JCS,100}}{2}$.

These equations show the importance of heat recovery efficiency. With the aforementioned $\Phi_{JCS,100}$ = 90% only 5% of Q gets lost with the exhaust air. At $\Phi_{JCS,100}$ = 80% it would be 10%. At the cost of this loss, which comes only with the JCSalso considerable savings are achieved. In [9] it is stated that the conveying energy for air heaters and air chillers will exceed this loss. Another saving comes from the enhanced efficiency.

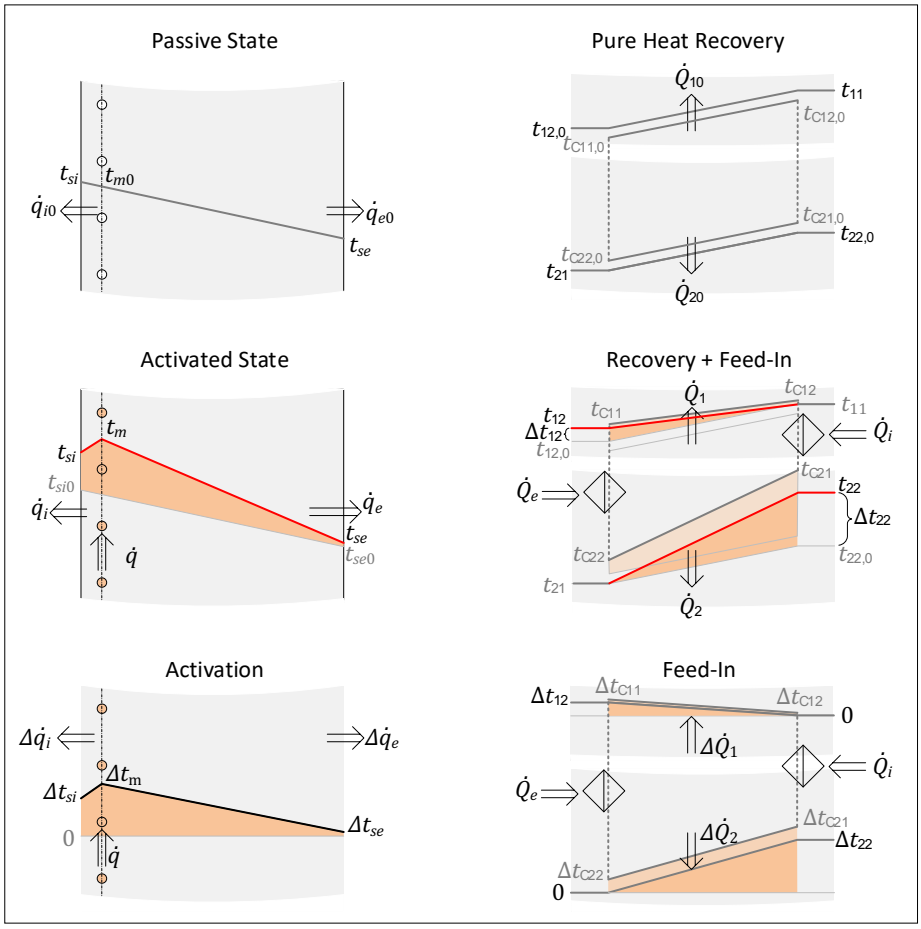

Figure 9: Similarities between thermoactive slabs and JCS with feed-In

The temperatures inside the circulation from the solution of equation (17) are

$$t_{C11} = \frac{\dot{Q}_e + \dot{Q}_i - \Phi_{100}\,\dot{Q}_i + \dot{C}_2\Phi_{100}\,t_{11} - \dot{C}_2\Phi_{100}{}^2\mathrm{t11} + \dot{C}_2\Phi_{100}\,t_{21}}{\dot{C}_2(2-\Phi_{100})\Phi_{100}}$$

$$t_{C12} = \frac{\dot{Q}_e - \Phi_{100}\,\dot{Q}_e + \dot{Q}_i - 2\Phi_{100}\,\dot{Q}_i + \Phi_{100}{}^2\dot{Q}_i + \dot{C}_2\Phi_{100}\,t_{11} + \dot{C}_2\Phi_{100}\,\mathrm{t21} - \dot{C}_2\Phi_{100}{}^2 t_{21}}{\dot{C}_2(2-\Phi_{100})\Phi_{100}}$$

$$t_{C21} = \frac{\dot{Q}_e - \Phi_{100}\,\dot{Q}_e + \dot{Q}_i + \dot{C}_2\Phi_{100}\,t_{11} + \dot{C}_2\Phi_{100}\,t_{21} - \dot{C}_2\Phi_{100}{}^2 t_{21}}{\dot{C}_2(2-\Phi_{100})\Phi_{100}}$$

$$t_{C22} = \frac{\dot{Q}_e - 2\Phi_{100}\,\dot{Q}_e + \Phi_{100}{}^2\dot{Q}_e + \dot{Q}_i - \Phi_{100}\,\dot{Q}_i + \dot{C}_2\Phi_{100}\,t_{11} - \dot{C}_2\Phi_{100}{}^2 t_{11} + \dot{C}_2\Phi_{100}\,t_{21}}{\dot{C}_2(2-\Phi_{100})\Phi_{100}}$$

For instance, at t_{21} = -10 °C, t_{11} = 20 °C, $\Phi_{JCS,100}$ = 90%, $\dot{C}_2$ = 3,000 W/K the heat flow from the recovery is $Q_{2,0}$ = 81 kW. The supply air temperature would be $t_{22,0}$ = 18.5 °C. With $\dot{Q}_i$ = 20 kW and $\dot{Q}_e$ = 40 kW it becomes t_{22} = 24.0 °C. The circulation temperatures at the inner link are t_{C12} = 19.2 °C and t_{C21} = 25.9 °C. If a heat pump delivered a supply temperature of 30 °C and the heat recovery coefficient at the inner link is Φ_{100} = 80%, its return temperature would be 21.4 °C which gives a much better performance than the heat pump would have, if it had to supply an air chiller with 60/40 or even 80/60. Moreover, 30 °C can also be delivered from a long-term storage.

At the outer link the circulation temperatures are t_{C22} = -8.1 °C and t_{C11} = 5.2 °C. At equal capacity flows on either side and NTU = 1 the temperature difference over the separating face is 13.3 K demanding a supply temperature of 5.2 °C which could be delivered from an anergy grid.

In the summer a supply air temperature t_{22} = 16.0 °C is reached at t_{11} = 26 °C and t_{21} = 32 °C with $\dot{Q}_i$ = - 33.5 kW and $\dot{Q}_e$ = 0. In this case the circulation temperatures at the inner link are t_{C12} = 26.3 °C and t_{C21} = 15.1 °C. With NTU = 4 at the inner link, according to Φ_{100} = 80%, the supply temperature would have to be 13.3 °C at equal capacity flows which could also be covered by an anergy grid as long as its temperature does not exceed this value which should be the case only atthe beginning of the cooling period.

Later on its about heating up the anergy grid for the heating period. This takes place also by extracting waste heat from the return air. In the example before the extracted heat would be 14.5 kW when the supply air temperature can reach t_{22}= 22.0 °C. Now, the circulation temperatures at the inner link would be t_{C12} = 26.3 °C and t_{C21} = 21.5 °C. With NTU = 4 the supply and return temperature from the grid would be 20.3 °C and 25.1 °C at equal capacity flows.

7. CONCLUSION AND PROSPECTS

Thermoactive building envelope technology as investigated widely during the last years can be complemented by joint circulation systems used as AHU´s operating with low temperature differences. The challenge in manufacturing lies in producing heat exchangers with very large separating faces, either by use of capillary tube mats or any other means that build up small parallel gaps with counterflow of air and water. The control of those systems is by no means trivial. Further investigations have to be made into it. With successful development large energy savings can be achieved in the future.

8. REFERENCES

[1] VDI 2071, 1997. Heat recovery in heating ventilation and air-conditioning plants (withdrawn)

[4] VDI 3525, 2007. Automation and control of air-conditioning systems – examples

[2] VDI 3803 sheet 5, 2013. Air-Conditioning System Requirements, Heat Recovery Systems

[5] Jüttemann H, 2001. Wärme- und Kälterückgewinnung in raumlufttechnischen Anlagen (Recovery of heating and cooling energy in in heating ventilationg and air conditioning plants)

[6] Kaup C, 2009. Mehrfachfunktionale Hochleistungs-Wärmerückgewinnungssysteme (Multi-functional high performance heat recovery systems): Heizung Lüftung Haustechnik

[7] Herbst D, 2008. Heat exchangers, method for use in an air conditioning system: Patent Specification DE 10 2008 034

[8] German Ministry of Science, 2011. ZIM-Project Enthalpy exchanger

[9] Kretschmer T, 2013. Wohin mit dem Erhitzer und Kühler bei Kreislaufverbundsystemen? (Where to install heater and chiller in joint circulation systems: Gesundheitsingenieur

[10] Kretschmer T, 2014. Optimale Wärmeübertrager - Laminar ist besser als turbulent (Optimal heat transfer – lamiminary ist better than turbulent): Gesundheitsingenieur

[11] Fraaß, M, 2015. Höhere Energieeffizienz mit Kreislaufverbundsystemen (Higher energy efficiency with joint circulation

systems): Heizung Lüftung Haustechnik

[12] Fraaß, M, 2007. Grundlagen des thermisch aktivierbaren Bauteils; Gesundheitsingenieur

[13] VDI, 2013. Wärmeatlas